Title
19F and 199Hg NMR of trimeric perfluoro-ortho-phenylenemercury

Journal
Journal of Molecular Structure, 839

Authors
Taylor, Robert E
Gabbai, Francois P

Publication Date
2007

DOI
10.1016/j.molstruc.2006.10.025

Peer reviewed

^{19}F and ^{199}Hg NMR of Trimeric Perfluoro-*ortho*-Phenylenemercury

R. E. Taylor[1*] and François P. Gabbaï[2*]

[1]Department of Chemistry and Biochemistry
University of California, Los Angeles
Los Angeles, CA 90095-1569 USA

[2] Department of Chemistry
Texas A&M University
College Station, TX 77843-3255 USA

Corresponding authors:
Email addresses: taylor@chem.ucla.edu (R. Taylor)
gabbai@mail.chem.tamu.edu (F. Gabbaï)

Abstract:

^{19}F and ^{199}Hg high-resolution solution NMR spectra were acquired for cyclic trimeric perfluoro-*ortho*-phenylenemercury. Even with the high superconducting magnetic fields currently available, the ^{19}F spectrum was not interpretable with a simple first-order analysis. Spectroscopic parameters for chemical shift and scalar coupling interactions in the NMR spectra were extracted from four- and five-spin simulations. Differential line widths in the ^{19}F spectrum result from scalar coupling to the ^{199}Hg.

Key Words:

NMR; ^{19}F NMR, ^{199}Hg NMR; Lewis acid; mercury; trimeric perfluoro-*ortho*-phenylenemercury; strong scalar coupling.

Introduction

Cyclic trimeric perfluoro-*ortho*-phenylene mercury (the "trimer") is a tridentate Lewis acid which complexes a number of neutral and anionic electron rich substrates and its chemistry has been recently reviewed [1,2]. The structure is shown in Figure 1. In the case of halides, complexation leads to the formation of adducts in which the halide anion forms secondary coordination bonds with the three mercury centers. A similar tridentate complexation is observed with the electron rich center of various donor substrates including organic carbonyls, nitriles, sulfoxides and dialkylsufides. Formation of these complexes substantiates the unusual Lewis acidic properties of the trimer**.** These properties result from the electron-withdrawing nature of the fluorinated backbone, the accessibility of the mercury centers as well as from cooperative effects arising from the proximity of the mercury(II) centers. Structural investigations also point to the propensity of this trinuclear derivative to engage in non-covalent interactions including mercuriophilic interactions and dispersion interactions [3]. For example, free trimer forms compact cofacial dimers whose structure has been determined by single crystal X-ray diffraction. As shown by recent developments, the trimer is also a remarkable supramolecular building block which readily forms binary stacks with various arenes including benzene and naphthalene [3,4]. The formation of these stacks, which results from secondary π interactions occurring between the mercury centers and the π-system of the arene, is likely assisted by attractive electrostatic and dispersion forces between the individual components.

For Nuclear Magnetic Resonance (NMR) spectroscopy, all nuclei present in this derivative are NMR-active and variation of their chemical shift upon addition of a substrate can sometime reflect adduct formation. This principle is nicely exemplified by the work of Shur and coworkers [5] who witness the complexation of electron rich substrates by ^{199}Hg NMR. For example, coordination of dimethylformamide to the trimer leads to a 12.3 ppm down field shift of the mercury resonance [6]. The fluorine nucleus constitutes another obvious NMR handle. As shown by Fackler and Burrini, the trimer forms binary stacks with trinuclear cyclic basic Au^I compounds such as $[Au(\mu\text{-}C^2,N^3\text{-bzim})]_3$ (bzim = 1-benzylimidazolate). Remarkably, a ^{19}F, ^{1}H-HOESY NMR measurement carried out on these adducts in THF-d_8 shows intermolecular cross-peaks of the adduct indicating that adducts between the trimer and $[Au(\mu\text{-}C^2,N^3\text{-bzim})]_3$ subsist in solution [7,8]. These two examples indicate that the NMR properties of the trimer are useful for monitoring and therefore understanding the chemistry of this tridentate Lewis acid. For these reasons, a detailed analysis of the NMR spectroscopic features of the trimer appears highly desirable.

Experimental

The ^{19}F NMR spectrum was acquired with a Bruker ARX-400 spectrometer at ambient temperature. One milligram of sample was dissolved in 0.5 ml of CD_2Cl_2 to minimize interaction between solute and solvent. The ^{19}F spectrum is referenced to an external sample of $CFCl_3$. The data were acquired with 512 scans using a 30 degree pulse every 5 seconds. A total of 128k time domain data points were acquired with a

spectral width of 21739.13 Hz, yielding a total acquisition time of 3.015 s for each scan. The size of the Fourier transform was 256k data points, yielding a digital resolution of 0.083 Hz/pt. The high sensitivity allowed resolution enhancement to be applied for the spectral analysis. One common method of resolution enhancement is the Lorentz-Gauss transformation [9]. This technique uses a negative line-broadening in Hertz to enhance the latter part of the free induction decay (FID) while using a second function to shift the point during acquisition when the FID reaches its maximum but forces the tail of the FID to zero. While this technique is implemented in many commercial software packages, it does suffer a drawback due to a decrease in the apparent signal-to-noise ratio (S/N).

The ^{199}Hg spectrum was acquired with a Bruker AV-600 spectrometer at ambient temperature. Nine milligrams of sample were dissolved in 0.5 ml of CD_2Cl_2. A total of 240,946 scans were acquired with a 90 degree pulse using a recycle delay of 100 ms. A total of 32k time domain data points were acquired with a spectral width of 53763.44 Hz, yielding a total acquisition time of 0.305 s for each scan. The size of the Fourier transform was 32k data points, yielding a digital resolution of 1.640 Hz/pt. The ^{199}Hg spectrum is referenced to $Hg(CH_3)_2$ at zero ppm by using an external sample of 1.0 M $HgCl_2$ in d-dimethylsufoxide assigned to -1501.0 ppm.

Spin-lattice T_1 relaxation times for both ^{19}F and ^{199}Hg were measured with the 180 - tau - 90 inversion recovery technique.

Attempts to observe the ^{201}Hg spectrum in the sample of 1.0 M $HgCl_2$ in d-dimethylsufoxide and in the trimeric perfluoro-*ortho*-phenylenemercury were unsuccessful.

Results and Discussion

The ^{19}F NMR spectrum of trimeric perfluoro-*ortho*-phenylenemercury, consisting of the two groups of resonances around -121.6 ppm and -155.7 ppm shown in Figure 2, has been described [5] as that of an AA'XX' spectrum, a four-spin problem. However, an analysis extracting the coupling constants was not reported. In those molecules showing coupling to the ^{199}Hg, this turns into a five-spin problem. Expansions of each group of resonances are shown in Figures 3 and 4. The ^{199}Hg spectrum, shown in Figure 5, of this compound was analyzed as a "triplet of triplets of triplets" [6] to report both the mercury shift and the Hg-F coupling constants. The full analyses of both the ^{19}F and ^{199}Hg spectra of this compound are presented in the following.

The spin-½ isotope ^{19}F is 100% naturally abundant while mercury has two NMR-active isotopes. The spin-½ isotope ^{199}Hg has a natural abundance of 16.84% while the spin-$^3/_2$ isotope ^{201}Hg has a natural abundance of 13.22%.

In the ^{19}F spectrum, the mercury satellites have a full width at half maximum (FWHM) of 9 Hz while the other ^{19}F resonances have a FWHM of 1 Hz. However, both the mercury satellites and the other ^{19}F resonances have the same spin-lattice T_1 relaxation time of 1.6 seconds within experimental error. The source of the differential line widths for these resonances is the scalar coupling to mercury. The measured ^{199}Hg spin-lattice T_1 relaxation time was 15 milliseconds. This short ^{199}Hg T_1 leads to the increased line width. No coupling to the ^{201}Hg isotope is observed in the ^{19}F spectrum, presumably due to an even shorter spin-lattice T_1 relaxation time for this quadrupolar

isotope. As a result, any ^{201}Hg scalar coupling can be ignored in the simulation if, due to the spin-lattice relaxation, the ^{201}Hg jumps from one spin state to another at a rate fast compared with the scalar coupling. Such fast ^{201}Hg spin-lattice relaxation would either broaden the coupled ^{19}F resonances beyond observation in this spectral window or, if sufficiently fast, in effect completely self-decouple the isotope from the ^{19}F nuclei.

NMR studies of ^{201}Hg itself are rare in the literature [10,11]. Even in solution the large quadrupole interaction provides a very efficient relaxation mechanism which results in resonance lines often broadened beyond observation. Although Wu and Wasylishen [11] reported the solid state ^{201}Hg spectrum for $K_2Hg(CN)_4$ in which the electric field gradient vanishes at the center of the $Hg(CN)_4$ tetrahedron, they pointed out that attempts to observe the ^{201}Hg signal from the same compound in solution were unsuccessful. They suggested that the ^{201}Hg T_1 is probably less than the probe dead time, which would explain the failure to directly observe the ^{201}Hg resonance. Additionally, such a short T_1 would explain the absence of any ^{201}Hg coupling in the ^{19}F spectrum of the trimer.

The four- and five-spin simulations of the ^{19}F and ^{199}Hg NMR spectra for the trimer were made with the Win-DAISY program [12]. The simulation model adds a ^{19}F simulation showing no coupling to mercury and a second ^{19}F simulation, appropriately scaled to reflect the natural abundance of ^{199}Hg, showing coupling to one ^{199}Hg atom. The model simulations of the ^{19}F resonances are shown in Figures 6 and 7. It should be noted that the model does not require any inter-ring ^{19}F coupling to accurately simulate the spectrum. The simulation of the ^{199}Hg spectrum, described earlier as a "triplet of triplets of triplets," requires coupling to the fluorines of two adjacent rings. The ^{19}F and ^{199}Hg chemical shifts and coupling constants from the simulations are tabulated in Table 1.

It should be noted that the $^3J(^{19}F\text{-}^{19}F)$ coupling constants of Table 1 are negative. This is consistent in sign with the three-bond coupling assignments of McFarlane [13] for perfluorodiphenyl mercury and perfluorophenylmercury acetate. While the one dimensional experiment cannot determine the signs of the coupling constants, the simulation is useful in illustrating that some coupling constants must be different in sign.

The ^{19}F spectrum of the compound can be simulated without any coupling to the ^{201}Hg nuclei. This result could arise from either the ^{19}F nuclei coupled to the ^{201}Hg being broadened beyond observation in this spectral window or from the ^{201}Hg nuclei self-decoupling from the ^{19}F nuclei. In an attempt to answer this question, the ^{19}F simulation model fit to the spectrum was integrated and gave the result that 26% of the total ^{19}F observed were coupled to ^{199}Hg nuclei.

Most mercury atoms (69.94%) are NMR-inactive, resulting in no coupling to the ^{19}F. Any scalar coupling would arise from the two NMR-active mercury isotopes, whose natural abundances were given earlier. With the compound having three mercury atoms per molecule, the permutations of the three mercury sites with the three types of mercury atoms can be used with the natural abundance to calculate the probabilities of the various molecules. Such a calculation shows that 34.95% of the molecules will have a single ^{199}Hg atom. However, as described above, the ^{199}Hg spectral simulation requires coupling to ^{19}F on only two of the three aromatic rings. As a result, such a model with complete observation of all ^{19}F nuclei due to the self-decoupling of the ^{201}Hg yields 23.3% of the ^{19}F coupled to ^{199}Hg while the remaining 76.7% of the ^{19}F is uncoupled to any mercury. Considering the small percentages of molecules with two or more ^{199}Hg

nuclei per molecule (which were not observed in the spectrum), this model with ^{201}Hg self-decoupling is in reasonable agreement with integration of the spectral simulation.

Unfortunately, this result does not answer unambiguously the question of whether the ^{19}F nuclei coupled to ^{201}Hg are simply broadened beyond observation or the ^{19}F nuclei are effectively decoupled from the ^{201}Hg and observed. For example, the percentage of molecules with one ^{199}Hg atom and no ^{201}Hg atoms is 24.72%. However, if ^{19}F coupled to ^{201}Hg is assumed to be broadened beyond observation in the spectrum, then only 24.6% of the observed fluorine would be coupled to the ^{199}Hg nuclei. Small errors in integration coupled with the small percentages of molecules having more than one ^{199}Hg atom per molecule (which are not observed in the spectrum) preclude determination of whether the ^{201}Hg effectively self-decouples from the ^{19}F or simply broadens the ^{19}F beyond observation in this window.

Strictly speaking, the designation as an AA'XX' spin system, requires an invariance in the spin interactions upon interchange of A and A' and of X and X'. Specifically, the chemical shift of A must be the same as A' and likewise for X and X'. Also, J_{AX} must equal $J_{A'X'}$ and $J_{AX'}$ must equal $J_{A'X}$. As can be seen from the ^{19}F coupling constants in Table 1, the fluorines in the trimer do not quite meet this strict criterion. For example, $J(F_1\text{-}F_4)$ of -23 Hz is not the same as $J(F_2\text{-}F_3)$ of -27 Hz. A better fit of the theoretical spectrum to the experimental is obtained when there is a two Hz difference in the chemical shifts of F_1 and F_2. This gives rise to the asymmetry in the theoretical peak intensities in each group of resonances, matching that seen in the experimental spectrum. (The asymmetry in peak intensities within each group of the experimental ^{19}F resonances is real and not simply due to insufficient digital resolution to fully characterize the line shapes.) This difference of two Hertz in the chemical shifts is smaller than the precision of the ^{19}F shifts given in Table 1. It is not certain if this shift difference is due to isotopic shifts arising from the mercury. Four such isotopic shifts arising from the various ^{35}Cl and ^{37}Cl ratios due to the differing natural abundances are clearly observed in the ^{19}F spectrum of $CFCl_3$ in high magnetic fields. Finally, it should be noted that the ^{19}F spin simulations are somewhat hampered by the broad peaks from the ^{199}Hg coupling obscuring some of the small amplitude ^{19}F transitions in the spectrum. This may lead to an increase in the error of the magnitudes of the coupling constants.

Conclusions

In the early days of NMR with the then typical magnets with proton frequencies of 30 and 40 MHz [14], full analysis of proton spectra frequently required accounting for strong scalar coupling. Even with the currently available superconducting magnets, examples of both ^{1}H spectra acquired at frequencies of 800 MHz [15] and ^{19}F spectra (with the ^{19}F chemical range of approximately 800 ppm) showing strong scalar coupling [16] still arise. The full analysis of spectra showing strong scalar coupling still finds application over fifty years after the solutions to these spectral problems were first reported in the literature, despite the technological progress made in constructing ever higher field NMR magnets.

The ^{19}F and ^{199}Hg NMR spectra for cyclic trimeric perfluoro-*ortho*-phenylenemercury were analyzed. The spectral simulations provided ^{199}Hg-^{19}F scalar coupling constants as

well as ^{19}F-^{19}F coupling constants. Those molecules in which ^{19}F nuclei show coupling to the ^{199}Hg nucleus exhibit a broader line width due to the short ^{199}Hg T_1 as compared with those molecules in which the ^{19}F show no coupling to mercury. ^{201}Hg nuclei show no coupling to the ^{19}F, either being effectively self-decoupled from the ^{19}F or simply broadening the coupled ^{19}F resonances beyond observation. Either explanation is presumably due to a very short spin-lattice relaxation time T_1 for the ^{201}Hg nuclei.

References

1. V. B. Shur, I.A. Tikhonova. Perfluorinated polymercuramacrocycles as anticrowns. Applications in catalysis. *Russian Chemical Bulletin (International Edition*) **52**(12) (2003) 2539-2554.

2. M.R. Haneline, R. E. Taylor, F. P. Gabbaï. Trimeric Perfluoro-*ortho*-phenylenemercury: A Versatile Lewis Acidic Host. *Chem. Eur. J.* **9** (2003) 5188-5193.

3. M.R. Haneline, M T.sunoda, F. P. Gabbaï. π-Complexation of Biphenyl, Naphthalene, and Triphenylene to Trimeric Perfluoro-*ortho*-phenylene Mercury. Formation of Extened Binary Stacks with Unusual Luminescent Properties. *J. Am. Chem. Soc.* **124** (2002) 3737-3742.

4. M. Tsunoda, F.P. Gabbaï. μ_6-η^2:η^2:η^2:η^2:η^2:η^2 As a New Bonding Mode for Benzene. *J. Am. Chem. Soc.* **122** (2000) 8335-8336.

5. V. B. Shur, I. A. Tikhonova, A. I Yanovsky, Y. T. Struchkov, P. V. Petrovskii, S. Y. Panov, G. G. Furin, M. E. Vol'pin. Crown compounds for anions. Unusual complex of trimeric perfluoro-*o*-phenylenemercury with the bromide anion having a polydecker sandwich strucure. *J. Organomet. Chem.* **418 (**1991) C29-C32.

6. I. A. Tikhonova, F. M. Dolgushin, K. I. Tugashov, P. V. Petrovskii, G. G. Furin, V. B. Shur. Coordination chemistry of polymercuramacrocycles. Complexation of cyclic trimeric perfluoro-*o*-phenylenemerucry with neutral oxygeneous Lewis bases. *J. Organomet. Chem.* **654** (2002) 123-131.

7. A . Burini, J. P. Fackler Jr., R . Galassi, T. A. Grant, M. A. Omary, M. A. Rawashdeh-Omary, B. R. Petroni, R. J. Staples. Supramolecular Chain Assemblies Formed by Interaction of a π Molecular Acid Complex of Mercury with π-Base Trinuclear Gold Complexes. *J. Am. Chem. Soc.* **122 (**2000) 11264-11265.

8. A. Burini, J. P. Fackler Jr., R. Galassi, A. Macchioni, M. A. Omary, M. A. Rawashdeh-Omary, B. R. Petroni, S. Sabatini, C. Zuccaccia. ^{19}F,^{1}H-HOESY and PGSE NMR Studies of Neutral Trinuclear Complexes of AU^{I} and Hg^{II}: Evidence for Acid-Base Stacking in Solution. *J. Am. Chem. Soc.* **124 (**2002) 4570-4571.

9. A. G. Ferrige, J. C. Lindon. Resolution Enhancement in FT NMR Through the Use of a Double Exponential Function. *J. Magn. Reson*. **31 (**1978) 337-340.

10. W. E. Blumberg, J. Eisinger, R. G. Shulman. Isotope Effect of Nuclear Magnetic Resonances in Metallic Mercury. *J. Phys. Chem. Solids* **26** (1965) 1187-1194.

11. G. Wu, R. E. Wasylishen. Observation of ^{201}Hg NMR Spectra for Solid $K_2Hg(CN)_4$. *Magn*. Reson. *Chem*. **31 (**1993) 537-539.

12. U. Weber, H. Thiele. *NMR-Spectroscopy: Modern Spectral Analysis*. Wiley-VCH: Weinheim, 1998.

13. W. McFarlane. A Magnetic Double Resonance Study of Some Aryl and Pentafluoroaryl Mercury Compounds. *J. Chem. Soc. (A)* (1968) 2280-2285.

14. R. Freeman. Pioneers of High-Resolution NMR. *Concepts Magn. Reson.* **11**(2) (1999) 61-70.

15. U. Weber, A. Germanus, H. Thiele. Modern strategies for PC-supported spectral analysis of 1D NMR data. *Fresenius J. Anal. Chem.* **359** (1997) 46-49.

16. M. Tschinkl, T. M. Cocker, R. E. Bachman, R. E. Taylor, F. P. Gabbaï. Synthesis and structure of fluorinated dialacycles. *J. Organometallic Chem.* **604** (2000) 132-136.

Table 1: ^{19}F and ^{199}Hg Chemical Shifts and Coupling Constants

	F_1	F_2	F_3	F_4	Hg
Chemical Shifts, ppm	-121.62	-121.62	-155.74	-155.74	-1048.3
Coupling Constants, Hz					
F_1		18.5	3.5	-27	393
F_2			-23	3.5	19
F_3				-15	103
F_4					19

^{19}F NMR chemical shifts relative to $CFCl_3$. ^{199}Hg NMR chemical shift relative to $Hg(CH_3)_2$. The positions of the fluorine atoms are shown in Figure 1.

A

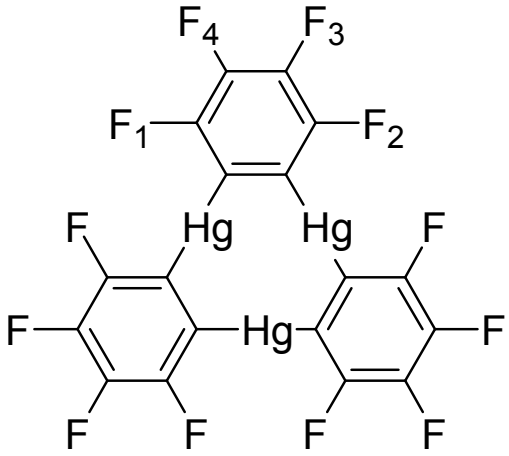

B

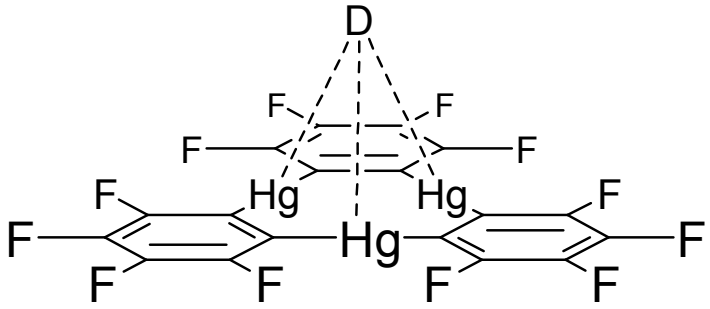

Figure 1: The structure of cyclic trimeric perfluoro-*ortho*-phenylenemercury is shown in A. For spectral assignments, the individual ^{19}F atoms in the above structure are subscripted one through four. The chemical shifts and coupling constants are given in Table 1. The general structures of the donor adducts of the trimer (D = donor) are shown in B.

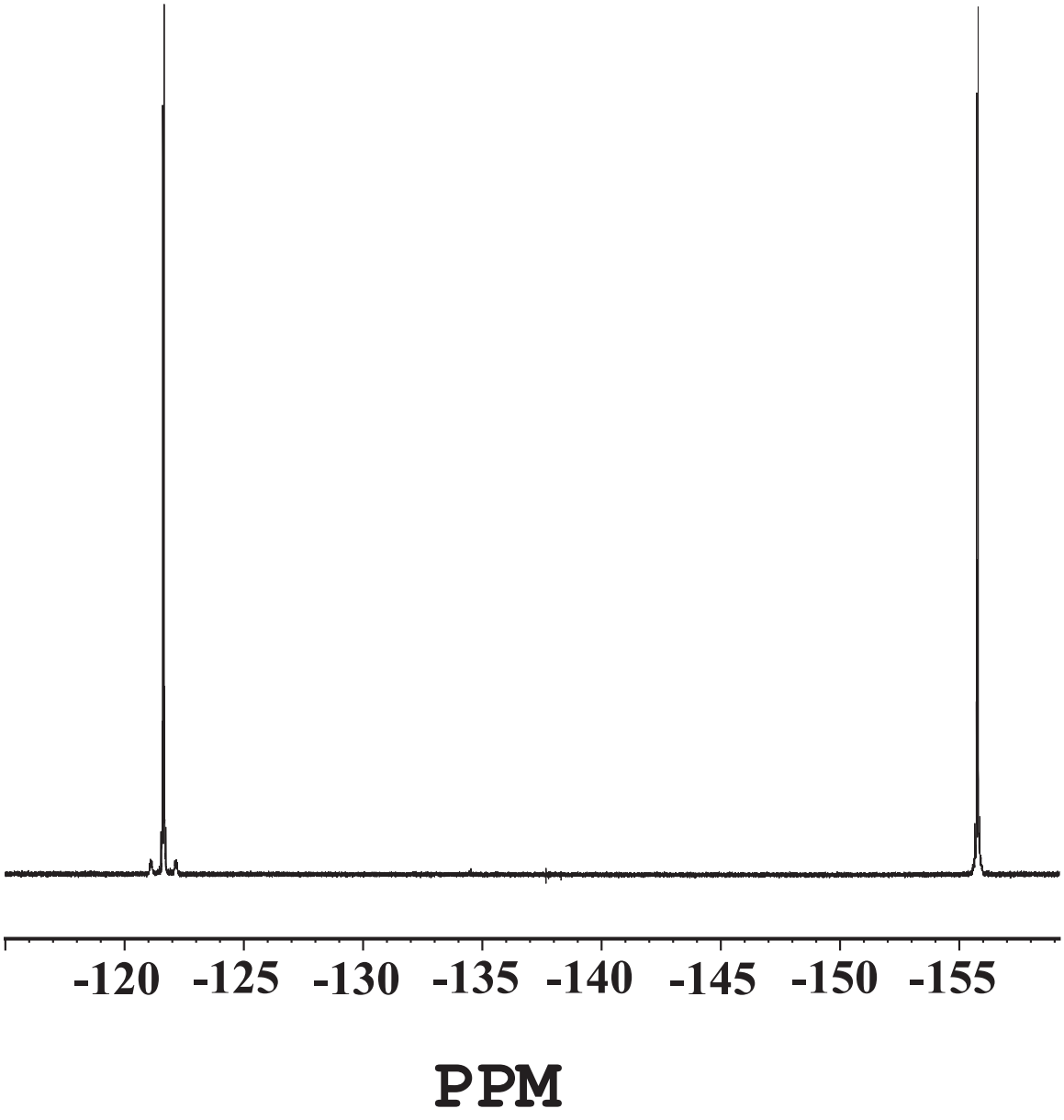

Figure 2: ^{19}F NMR spectrum of cyclic trimeric perfluoro-*ortho*-phenylenemercury.

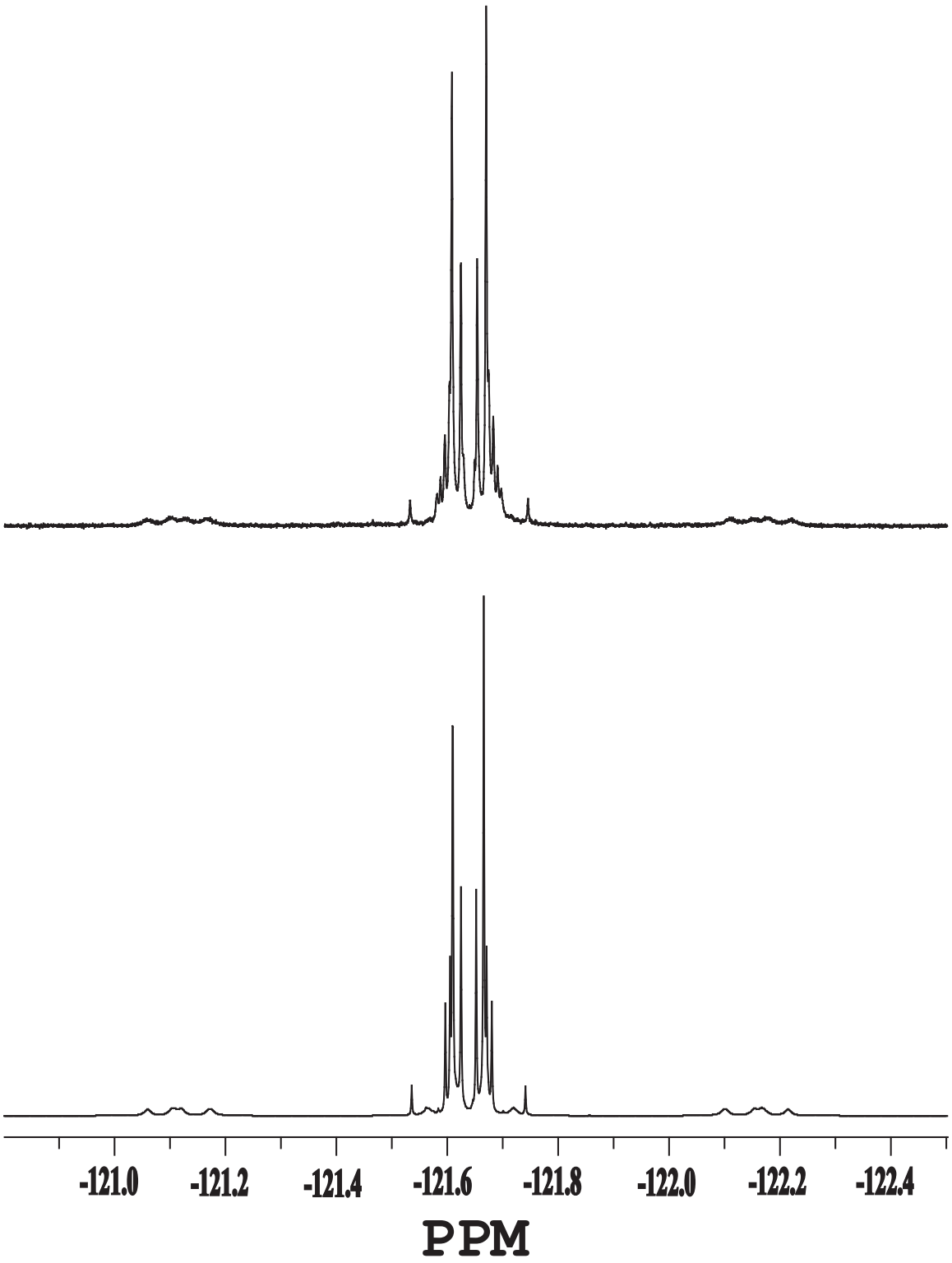

Figure 3: ^{19}F NMR experimental spectrum (top) and simulation (bottom) of F_1 and F_2 as labeled in the structure of cyclic trimeric perfluoro-*ortho*-phenylenemercury given in Figure 1.

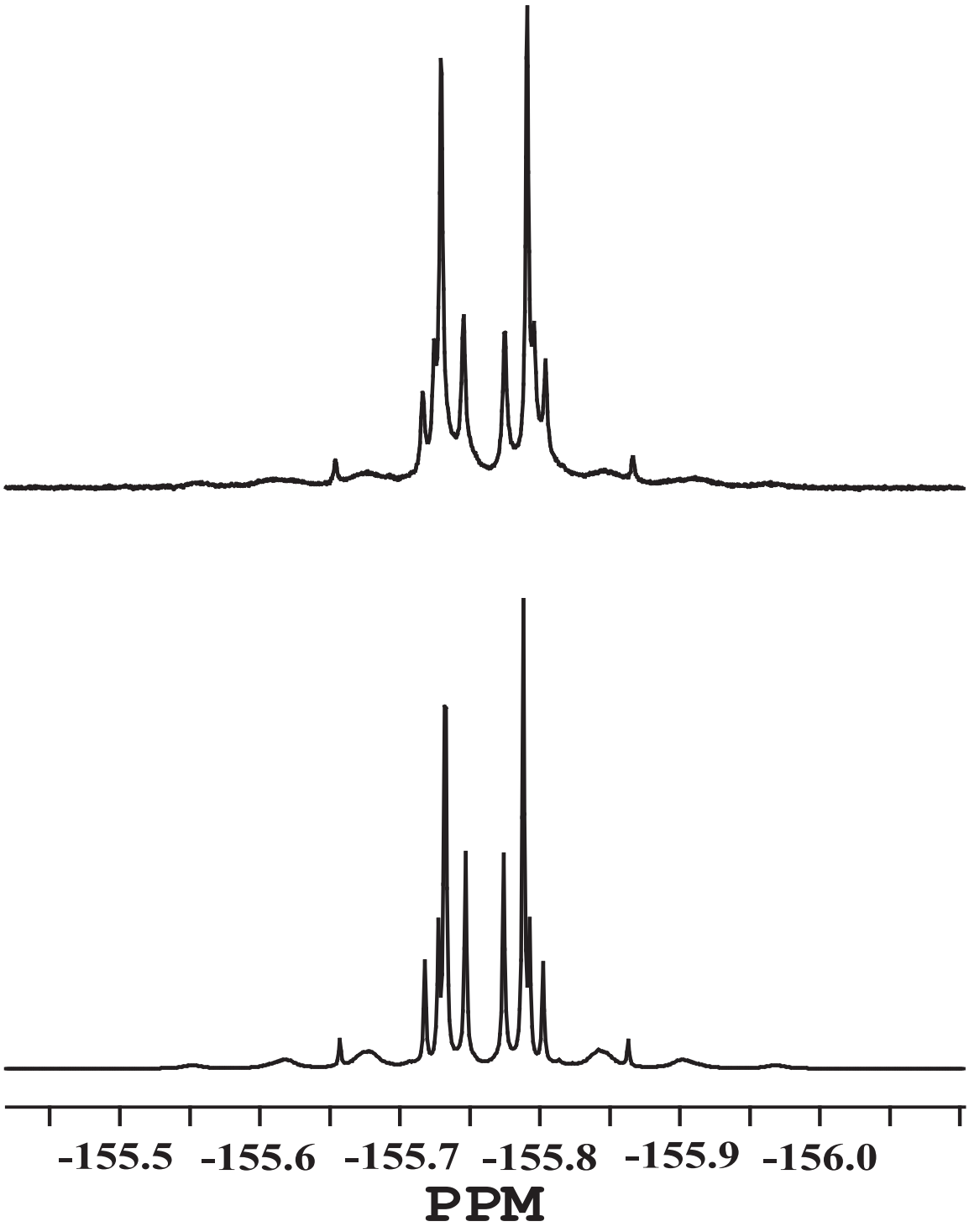

Figure 4: ^{19}F NMR experimental spectrum (top) and simulation (bottom) of F_3 and F_4 as labeled in the structure of cyclic trimeric perfluoro-*ortho*-phenylenemercury given in Figure 1.

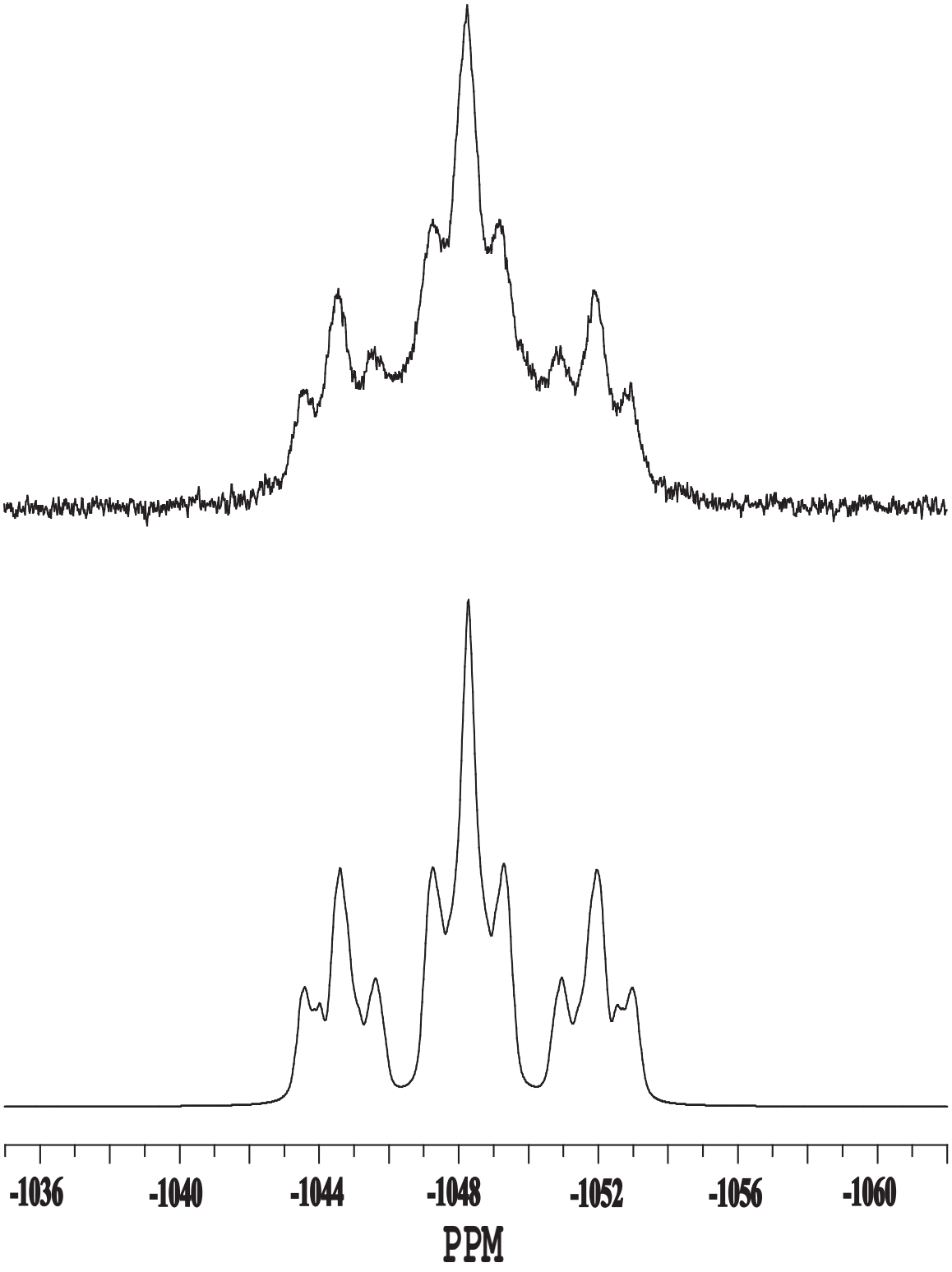

Figure 5: ^{199}Hg NMR experimental spectrum (top) and simulation (bottom) of cyclic trimeric perfluoro-*ortho*-phenylenemercury.

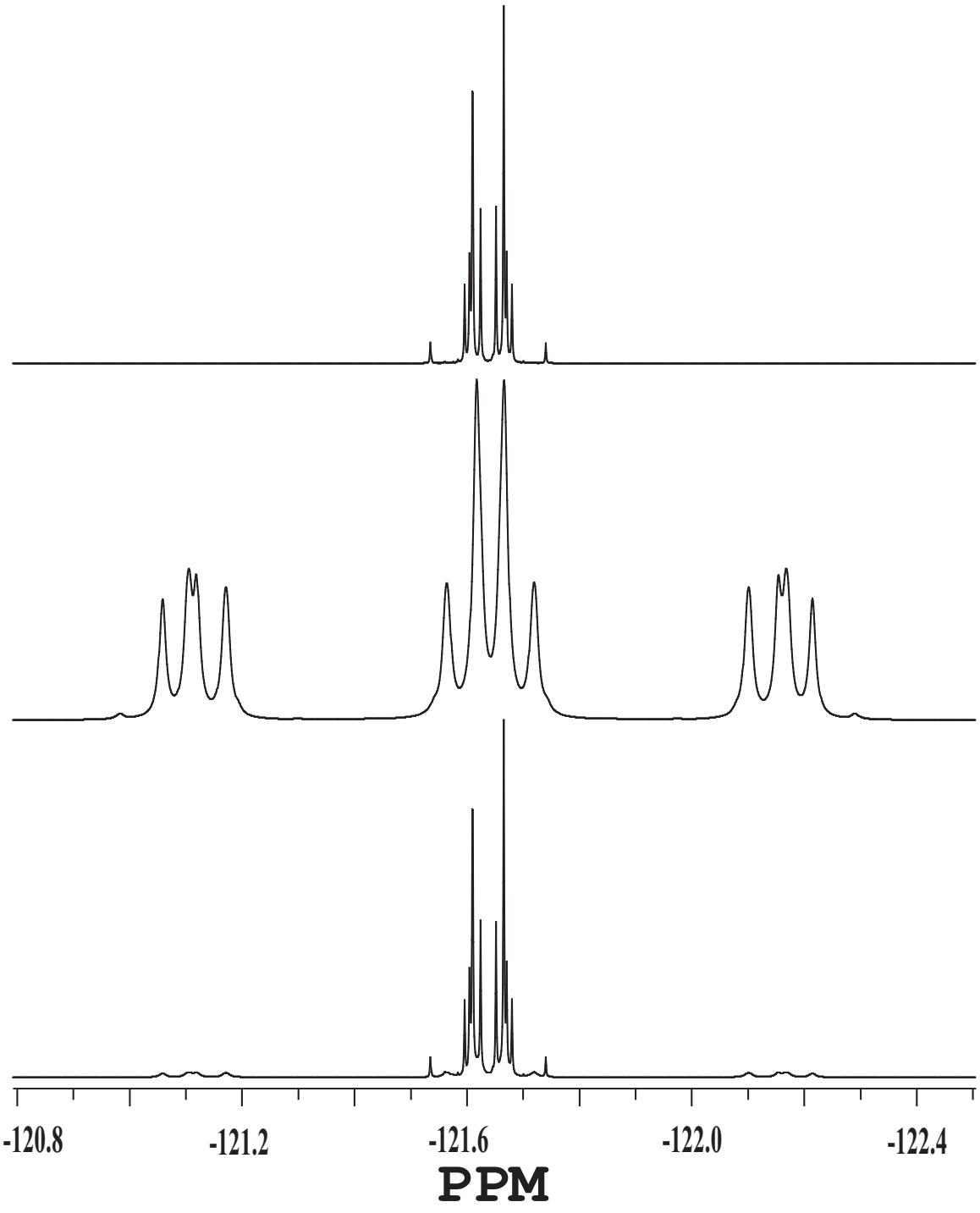

Figure 6: The simulation model (bottom) results from the addition of the ^{19}F simulation with no mercury couplings (top) added to the ^{19}F simulation with coupling to one ^{199}Hg atom (middle) scaled to reflect the natural abundance of ^{199}Hg.

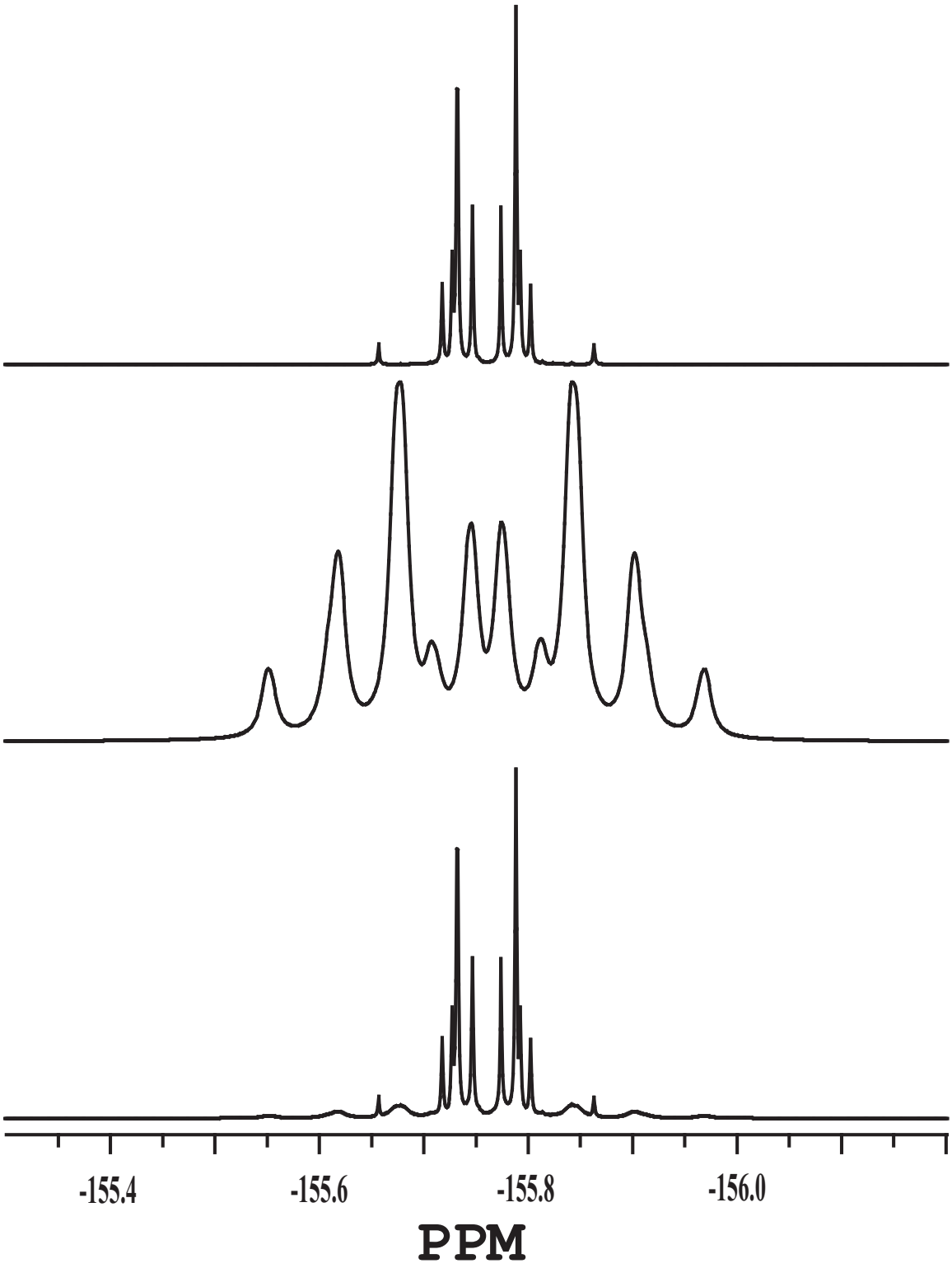

Figure 7: The simulation model (bottom) results from the addition of the ^{19}F simulation with no mercury couplings (top) added to the ^{19}F simulation with coupling to one ^{199}Hg atom (middle) scaled to reflect the natural abundance of ^{199}Hg.